Removal of As(V) from groundwater by a new electrocoagulation reactor using Fe ball anodes: optimization of operating parameters

E. Sık[a], M. Kobya[b,*], E. Demirbas[a], M.S. Oncel[b], A.Y. Goren[b]

[a]*Department of Environmental Engineering, Gebze Institute of Technology, 41400 Gebze, Turkey*
[b]*Department of Chemistry, Gebze Institute of Technology, 41400 Gebze, Turkey, Tel. +90 262 6053214; Fax: +90 262 6538490;*
email: kobya@gyte.edu.tr (M. Kobya)

ABSTRACT

Removal of As(V) from groundwater by a new air-injected electrocoagulation (EC) reactor using iron (Fe) ball anodes was investigated and the operating conditions were optimized. Effects of operating parameters such as initial pH (pH_i: 6.5–8.5), current (i: 0.1–0.5 A), operating time (t_{EC}: 1–3 min), size of Fe anode ball (d_p: 5–10 mm), initial As(V) concentration (C_o: 50–150 μg/L), air flow rate (Q_{air}: 2–10 L/min), and column height of Fe ball (h: 2–8 cm) in the EC reactor were evaluated with a three-level factorial design viz. Box–Behnken statistical experiment design. The model program provided with responses such as effluent As(V) concentration, removal efficiency, and operating cost for the EC process. Analysis of variance for all variables had confirmed the predicted models by the experimental design within 95% confidence level (R^2: 0.94, adj-R^2: 0.87), which ensured a satisfactory adjustment of the quadratic model with the experimental data. The maximum removal efficiency of As(V), minimum operating cost, and lowest effluent concentration at the optimized conditions (pH_i 7.2, 0.5 A, 1.2 min, 5 mm ball size, column height of 4.8 cm, and 9.9 L/min) for initial concentration of 100 μg/L were obtained as 99.2%, 0.031 \$/m³, and 0.4 μg/L, respectively.

Keywords: Arsenate removal; Electrocoagulation; Iron ball anode; Optimization

1. Introduction

Arsenic is one of the well-known toxic elements in the world. It is a poisonous substance, invisible, tasteless, and odorless. Arsenic concentration in water can become elevated due to several reasons such as, mineral dissolution, use of arsenical pesticides, disposal of fly ash, mine drainage, and geothermal discharge [1]. Contamination of groundwater with arsenic is a major environmental and public health problem on a global scale. Higher concentrations of arsenic are observed in many countries including Bangladesh, India, China, Taiwan, USA, Canada Mexico, Chile, Argentina, Croatia, New Zealand, Hungary, Turkey, and Vietnam [2,3]. Exposure to high levels of arsenic can cause problems in humans such as gastrointestinal, hematologic, hepatic, renal, skin lesions, hyperkeratosis, neurologic, and immunologic effects [4]. Therefore, the World Health Organization (WHO) has set a value for drinking water production of 10 μg/L [5].

*Corresponding author.

Turkey is one of the countries under the threat of arsenic pollution and numerous cases of arsenic contamination in groundwater. Surface waters have also been reported and concentrations are ranging from 0.5 to 10,700 µg/L in Turkey within the last 10 years [6–8]. Consequently, natural waters of some regions of Turkey pose a potential threat to the community health regarding the concentration of arsenic according to new maximum contaminant level set by the WHO.

In this study, electrocoagulation (EC) process was used for the removal of arsenic from groundwater since EC was capable of removing arsenic to trace levels, simple in operation, compact treatment facility, cost-effective, and no need to handle chemicals [9,10]. The EC process has also advantage of removing the smaller colloidal particles and producing relatively low amount of sludge. This method has been successfully applied for the treatment of various industrial wastewaters [11–25]. Plate and rod types of Al or Fe anode electrodes were generally used in the EC reactors and these had some disadvantages namely, time consuming (changing and maintenance) and accommodate a limited number of plate and rod types of electrodes with low surface areas. For that reason, an air-injected new EC reactor was designed to eliminate the above problems. The new EC reactor has specifications of compactness, easy to use, accommodating of more anode electrodes with higher surface areas, and providing better removal efficiency of As(V) from groundwater. Therefore, the new air injected EC reactor using Fe ball anodes is needed to be optimized for the optimum operating conditions.

The aim of the present study was to remove As(V) concentration in the range 50–150 µg/L from groundwater by the new air-injected EC reactor using iron ball anode electrodes. Effects of operating parameters (initial pH, applied current, operating time, size of iron ball anode, initial As(V) concentration, air flow rate, and height of anode in the reactor) were evaluated to determine the optimum levels of the factors that significantly influence removal efficiency, effluent concentration, and operating cost by the three-level Box–Behnken experimental design (Design Expert 8.0.4.1 trial version). The technique could improve the removal efficiency and provide closer confirmation of the output response toward the target requirements.

2. Materials and methods

2.1. Groundwater characteristics

Groundwater for the EC experiments was obtained from a well situated in the province of Kocaeli in Turkey and stored in five tones high-density polyethylene container. Characterizations of the groundwater were shown in Table 1. All chemical species present in groundwater were determined with standard methods [26]. The concentrations of cations such as Ca, Mg, Mn, Na, and Si by ICP optical emission spectrometry and anions such as nitrate, sulfate, and chloride by ion chromatography (Shimadzu HIC-20A) were measured for the groundwater. TOC and turbidity were determined by TOC analyzer (Tekmar Dohrmann, Apollo 9000) and turbid meter (Hach Lange DR 2800). Total dissolved solid was measured by Mettler Toledo Seven Go. Fe, Al, P, F, and As in the groundwater were not detected. The groundwater samples were daily prepared in the concentration range 50–150 µg/L by $Na_2HAsO_4 \cdot 7H_2O$.

2.2. The air injected EC reactor

The new EC reactor with an air-injection unit was designed for removal of As(V) from groundwater (Fig. 1). The EC reactor consisted of a round bottom base unit (150 mm in diameter and 45 mm in thickness) having a number of round holes in 2 mm diameter drilled with equidistant and a direct air was supplied underneath with a compressor. An air feed diffuser was attached underneath the base unit. A Plexiglas in a cylindrical shape ($245 \times 100 \times 5$ mm) was fixed to the base unit and another cylindrical shaped titanium cathode material ($250 \times 70 \times 1$ mm) with 5 mm in diameter holes drilled in equidistant (10 mm intervals) all over the length was inserted inside the Plexiglas cylinder ($250 \times 60 \times 5$ mm). Second Plexiglas with 2 mm in diameter drilled holes over the length was placed inside the cathode and filled with Fe ball anode materials (purity > 99.5%) with size of 2–8 mm

Table 1
Characterizations of the groundwater

Parameters	Value
pH	7.6
Conductivity (µS/cm)	1055.0
Total suspended solids (mg/L)	528.0
Total organic carbon (mg/L)	5.0
Turbidity (NTU)	1.0
Total alkalinity (CaCO$_3$, mg/L)	260.0
Total hardness (CaCO$_3$, mg/L)	418.0
Mn^{2+} (mg/L)	0.006
Na$^+$ (mg/L)	22.0
Ca^{2+} (mg/L)	152.0
Mg^{2+} (mg/L)	15.0
Si (mg/L)	10.2
Cl$^-$ (mg/L)	127.0
SO$_4^{2-}$ (mg/L)	94.2
NO$_3^-$ (mg/L)	24.0

Bottom view of the air diffuser unit
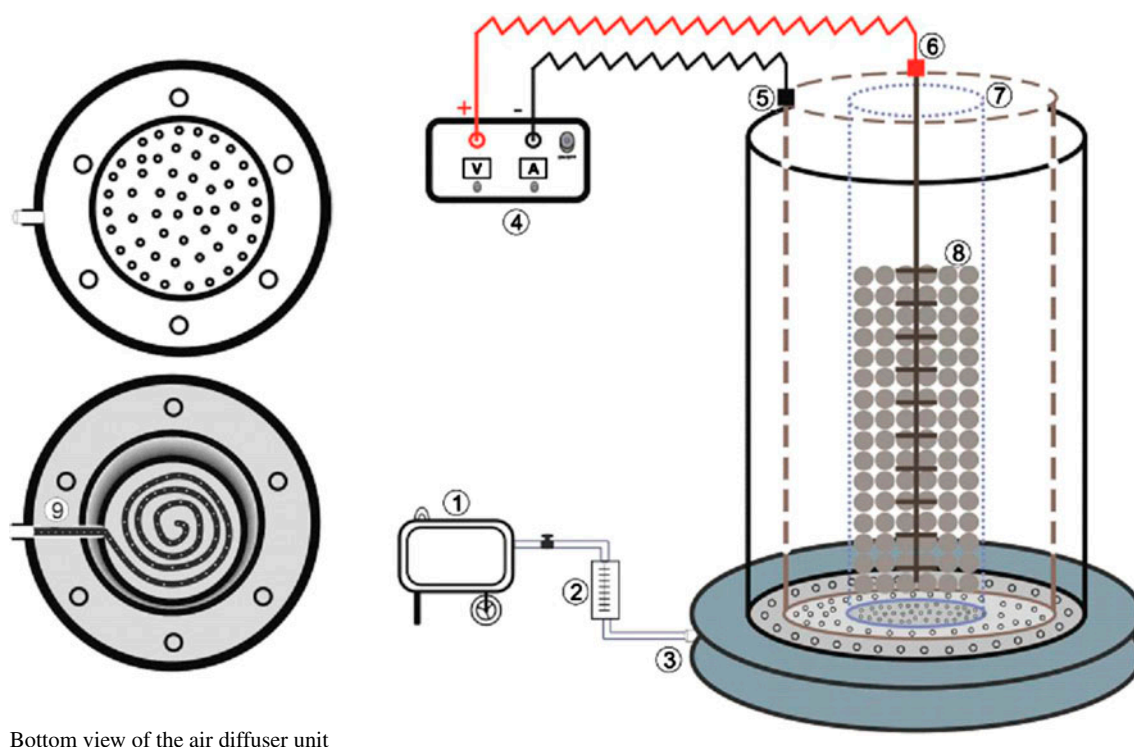
Fig. 1. A schematic diagram of an air fed EC reactor (1. Air compressor, 2. Air flow meter, 3. Air diffuser line, 4. DC power supply, 5. Cylindrical Ti cathode, 6. Supporting rod for Fe anode, 7. Inner cylindrical Plexiglas, 8. Anode Fe balls, 9. Air diffuser unit).

up to 80 mm in height. The titanium cylinder as a cathode was connected to the negative outlet of a DC power supply (Agilent 6675A model). A stainless steel rod (260 mm in length and 2 mm in diameter) was immersed in center of Fe ball anodes and connected to the positive outlet of the DC power supply. The anode materials had a higher surface area due to its shape.

2.3. Experimental design

The Box–Behnken experimental design method was used to determine the effects of major operating variables on As(V) removal and to find the combination of variables resulting in maximum As(V) removal efficiency. The Design Expert 8.0.4.1 trial version program (USA) was used for the statistical design of experiments and data analysis. The factorial design helped to develop a statistical model of a reaction by performing the minimum number of well-chosen experiments and to determine the optimal values of process parameters. Sixty-two experiments were carried out in the EC process for the removal of As(V) as required from the design procedure (Table 2). The independent variables range and levels were given in Table 3. The

experimental design involved seven operating variables, each at three levels and coded (−1), (0), and (+1) for low, middle, and high, respectively (Table 2). Three dependent parameters were analyzed as responses; effluent arsenic concentration (C_f, µg/L), arsenic removal efficiency (R_e, %), and operating cost (OC, $/m^3$) for the removal of arsenic from groundwater in the EC process (Table 2).

2.4. Analytical methods

An amount of 0.8 L of the groundwater containing As(V) was placed into the EC reactor. Then, Fe anode balls were filled to the required height in the EC reactor, after organic impurities and oxide layer on electrode surfaces were removed by dipping for 2 min in a solution freshly prepared by mixing HCl (35%) and hexamethylenetetramine aqueous solutions (2.80%) [11]. Current and voltage were held constant at desired values for each experimental run. pH of the solutions was adjusted by 0.1 N NaOH or 0.1 N H_2SO_4. pH and conductivity of solutions before and after the EC process were measured by a pH meter (Mettler Toledo Seven Compact) and a conductivity meter (Mettler Toledo Seven Go), respectively.

Table 2
A full factorial design of seven independent variables along with responses for the removal of As(V) from groundwater

Exp.	pH_i (−)	i (A)	t_{EC} (min)	d_p (mm)	C_o (µg/L)	h (cm)	Q_{air} (L/min)	C_f (µg/L)	OC ($/m^3$)	R_e (%)
1	7.5	0.5	1.0	7.5	100	2.0	6.0	4.84	0.057	95.2
2	8.5	0.3	2.0	7.5	100	8.0	2.0	7.61	0.123	92.4
3	8.5	0.5	2.0	5.0	100	5.0	6.0	0.65	0.117	99.4
4	7.5	0.1	2.0	7.5	150	5.0	2.0	6.61	0.113	95.6
5	7.5	0.3	1.0	5.0	100	5.0	2.0	29.18	0.036	70.8
6	7.5	0.3	3.0	10.0	100	5.0	2.0	8.62	0.174	91.4
7	6.5	0.3	2.0	7.5	100	2.0	2.0	23.01	0.093	77.1
8	7.5	0.3	1.0	5.0	100	5.0	10.0	4.63	0.054	95.4
9	6.5	0.1	2.0	5.0	100	5.0	6.0	21.01	0.183	79.1
10	6.5	0.5	2.0	5.0	100	5.0	6.0	0.45	0.029	99.6
11	8.5	0.1	2.0	10.0	100	5.0	6.0	13.53	0.098	86.5
12	6.5	0.1	2.0	10.0	100	5.0	6.0	16.47	0.187	83.5
13	7.5	0.3	2.0	5.0	50	2.0	6.0	0.84	0.051	98.3
14	7.5	0.3	1.0	10.0	100	5.0	10.0	16.01	0.098	84.1
15	7.5	0.3	3.0	5.0	100	5.0	2.0	0.52	0.289	99.5
16	8.5	0.3	1.0	7.5	50	5.0	6.0	0.89	0.077	98.2
17	7.5	0.5	1.0	7.5	100	8.0	6.0	8.38	0.053	91.6
18	8.5	0.3	2.0	7.5	100	2.0	10.0	6.71	0.146	93.3
19	6.5	0.3	2.0	7.5	100	2.0	10.0	5.92	0.120	94.1
20	6.5	0.3	3.0	7.5	150	5.0	6.0	0.59	0.215	99.6
21	7.5	0.1	2.0	7.5	150	5.0	10.0	25.22	0.117	83.2
22	7.5	0.5	3.0	7.5	100	2.0	6.0	0.43	0.273	99.6
23	7.5	0.3	2.0	5.0	50	8.0	6.0	2.39	0.078	95.2
24	7.5	0.3	2.0	7.5	100	5.0	6.0	3.67	0.102	96.3
25	8.5	0.5	2.0	10.0	100	5.0	6.0	2.38	0.160	97.6
26	6.5	0.3	2.0	7.5	100	8.0	10.0	6.43	0.121	93.6
27	7.5	0.5	2.0	7.5	150	5.0	2.0	8.62	0.098	94.3
28	7.5	0.3	2.0	7.5	100	5.0	6.0	2.78	0.174	97.2
29	7.5	0.3	2.0	10.0	150	2.0	6.0	9.47	0.053	93.7
30	8.5	0.3	3.0	7.5	150	5.0	6.0	2.39	0.186	98.4
31	7.5	0.3	2.0	10.0	150	8.0	6.0	8.38	0.173	94.3
32	6.5	0.3	3.0	7.5	50	5.0	6.0	0.63	0.183	98.7
33	8.5	0.1	2.0	5.0	100	5.0	6.0	7.29	0.127	92.7
34	7.5	0.3	2.0	10.0	50	8.0	6.0	1.62	0.112	96.8
35	7.5	0.3	2.0	7.5	100	5.0	6.0	3.41	0.100	96.6
36	7.5	0.5	2.0	7.5	150	5.0	10.0	2.54	0.234	98.3
37	7.5	0.3	3.0	5.0	100	5.0	10.0	9.52	0.180	90.5
38	7.5	0.3	2.0	7.5	100	5.0	6.0	4.03	0.121	96.1
39	7.5	0.5	2.0	7.5	50	5.0	2.0	0.52	0.030	99.1
40	7.5	0.3	3.0	10.0	100	5.0	10.0	0.71	0.175	99.3
41	7.5	0.5	2.0	7.5	50	5.0	10.0	0.63	0.111	98.7
42	7.5	0.1	2.0	7.5	50	5.0	2.0	4.64	0.151	90.7
43	7.5	0.3	2.0	5.0	150	8.0	6.0	1.51	0.180	99.1
44	7.5	0.1	1.0	7.5	100	2.0	6.0	39.55	0.084	60.5
45	7.5	0.3	2.0	10.0	50	2.0	6.0	4.59	0.157	90.8
46	8.5	0.3	2.0	7.5	100	8.0	10.0	1.48	0.134	98.5
47	7.5	0.3	2.0	7.5	100	5.0	6.0	3.51	0.175	96.5
48	7.5	0.3	1.0	10.0	100	5.0	2.0	9.51	0.060	90.5
49	6.5	0.3	1.0	7.5	150	5.0	6.0	24.36	0.109	83.8
50	6.5	0.3	2.0	7.5	100	8.0	2.0	23.01	0.047	77.1
51	6.5	0.5	2.0	10.0	100	5.0	6.0	3.75	0.126	96.3
52	8.5	0.3	2.0	7.5	100	2.0	2.0	7.01	0.057	93.1

(*Continued*)

Table 2
(*Continued*)

Exp.	pH$_i$ (−)	i (A)	t_{EC} (min)	d_p (mm)	C_o (µg/L)	h (cm)	Q_{air} (L/min)	C_f (µg/L)	OC ($/m^3)	R_e (%)
53	7.5	0.1	1.0	7.5	100	8.0	6.0	29.18	0.056	70.8
54	6.5	0.3	1.0	7.5	50	5.0	6.0	11.14	0.031	77.7
55	7.5	0.3	2.0	7.5	100	5.0	6.0	5.36	0.137	94.6
56	7.5	0.1	3.0	7.5	100	2.0	6.0	16.55	0.106	83.5
57	7.5	0.5	3.0	7.5	100	8.0	6.0	0.49	0.285	99.5
58	8.5	0.3	3.0	7.5	50	5.0	6.0	1.65	0.192	96.7
59	7.5	0.1	2.0	7.5	50	5.0	10.0	8.57	0.045	82.9
60	7.5	0.3	2.0	5.0	150	2.0	6.0	13.14	0.102	91.2
61	8.5	0.3	1.0	7.5	150	5.0	6.0	13.64	0.098	90.9
62	7.5	0.1	3.0	7.5	100	8.0	6.0	4.72	0.066	95.3

Table 3
Independent variables and their levels in the Box–Behnken statistical experiment design

Independent variables	Range and levels (coded)		
	Low −1	Center 0	High +1
x_1: initial pH (pH$_i$)	6.5	7.5	8.5
x_2: applied current (i, A)	0.1	0.3	0.5
x_3: EC time (t_{EC}, min)	1	2	3
x_4: size of Fe anode ball (d_p, mm)	5.0	7.5	10.0
x_5: as(V) concentration (C_o, µg/L)	50	100	150
x_6: anode height in the reactor (h, mm)	20	50	80
x_7: air flow rate (Q_{air}, L/min)	2	6	10

The samples taken from the EC reactor at different operating times were filtered using a 0.45 µm Millipore membrane filter. The hydride generation procedure coupled with ICP optical emission spectrometer (PerkinElmer Optima 7,000 DV model) was used to determine the total arsenic concentration in the sample at 188.9 nm. The detection limit for this study was 0.1 µg/L of As(V). All the experiments were repeated three times and the average data were reported.

2.5. Energy and electrode consumptions

The energy and electrode consumptions are extremely important parameters in the EC process as in all other electrolytic processes. The specific electrical energy consumption (ENC, kWh/m^3) for the solution is calculated from the following equation

$$\text{ENC}\,(\text{kWh/m}^3) = \frac{U \times i \times t_{EC}}{v} \tag{1}$$

where U is cell voltage (V), i is current (A), t_{EC} is operating time (h), and v is volume (m^3) of solution. The maximum possible mass of iron dissolved electrochemically from the anode for a particular electrical current flow in an electrolytic cell is quantified by Faraday's law (Eq. (2)).

$$\text{ELC}(\text{kg/m}^3) = \frac{i \times t_{EC} \times M_w}{z \times F \times v} \tag{2}$$

where ELC is the amount of anode material dissolved (kg/m^3), t_{EC} is operating time (s), M_W is molecular mass of iron (55.98 g/mol), z is the number of electrons transferred ($z = 2$), F is Faraday's constant (96487 C/mol), and v is volume of solution (m^3).

The operating cost (OC, $/m^3) in the EC process included electrodes and electrical energy costs, labor, maintenance, chemicals, sludge dewatering, disposal, and fixed costs [27,28]. In this study, energy and electrode material costs were taken into account as major cost items for the calculation of OC:

$$\text{OC} = \alpha \times \text{ENC} + \beta \times \text{ELC} \tag{3}$$

where α and β are values of electrical energy price (0.19 $/kWh) and electrode material price (4.5 $/kg Fe) provided by Turkish market in July 2013.

3. Arsenic removal mechanism with EC

EC generates metallic hydroxide flocs *in situ* by electrodissolution of soluble anode material. The production of metal cations from the anode and other charged metal hydroxide species may cause neutralization of negatively charged particles [9,22,23]. Then, the particles in solution bind together to form flocs, which result in the removal of pollutant from wastewater. When charge is applied through an external power source, the electrolytic dissolution of sacrificial

anode produces the cationic monomeric species according to the following equations:

Anodic reactions:

$$4Fe_{(s)} \rightarrow 4Fe^{2+} + 8e^- \tag{4}$$

$$4Fe_{(s)} \rightarrow 4Fe^{3+} + 12e^- \tag{5}$$

$$Fe^{2+} \rightarrow 4Fe^{3+} + e^- \tag{6}$$

Cathodic reactions:

The increase in pH during EC was primarily attributed to the increase in hydroxide ions (OH^-) concentration in solution resulting from water reduction at cathode.

$$2H_2O + 2e^- \rightarrow H_{2(g)} + 2OH^- \tag{7}$$

$$8H^+_{(aq)} + 8e^- \rightarrow 4H_2 \tag{8}$$
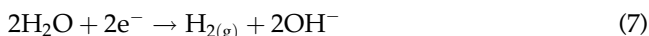
Reactions 7 and 8 for water oxidation increase pH value of the solution. Additionally, precipitation of ferric hydroxides decreases the pH value of the solution, as indicated by Eq. (10). Although iron is released as Fe^{2+}, it is rapidly oxidized to Fe^{3+} by dissolved oxygen in the solution. Oxidation of 1 mol of Fe^{2+} consumes 1 mol of H^+, as indicated by

$$O_{2(g)} + 4Fe^{2+} + 4H^+ \rightarrow 4Fe^{3+} + 2H_2O \tag{9}$$
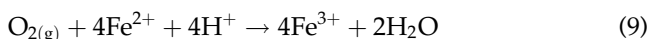
Generally, Fe^{3+} ions released from anode are gradually hydrolyzed and forms $Fe(OH)_{3(s)}$, if there is no other reactive species in solution. The rate of the oxidation depends on the availability of dissolved oxygen. Typically at the cathode, the solution becomes alkaline with time. The applied current forces OH^- ion migration towards the anode, thus favoring ferric hydroxide formation (Eq. (10)):

$$Fe^{3+} + 3OH^- \rightarrow Fe(OH)_{3(s)} \tag{10}$$
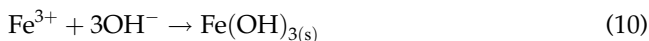
Ferric ions generated by electrochemical oxidation of iron electrode may form monomeric species with respect to pH of the medium, $Fe(OH)_3$, and polymeric hydroxyl complexes such as $Fe(OH)^{2+}$, $Fe(OH)_2^+$, $Fe_2(OH)_2^{4+}$, $Fe(OH)_4^-$, $Fe(H_2O)_2^+$, $Fe(H_2O)_5OH^{2+}$, $Fe(H_2O)_4(OH)_2^+$, $Fe(H_2O)_8(OH)_2^{4+}$, and $Fe_2(H_2O)_6(OH)_4^{2+}$. These hydroxides/polyhydroxides iron compounds have strong affinity for dispersed particles. As pH in the EC process is held on a fixed value, OH^- ions released from the cathode are totally consumed by Fe^{3+}

ions. Iron is dissolved giving rise to ferrous ions and its oxidation occurs by the following reaction.

$$Fe^{2+} + 3OH^- \rightarrow FeOOH + H_2O + e \tag{11}$$
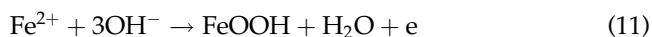
FeOOH produced in the EC has an isoelectric pH of about 7.0. Below this pH, the surfaces of the particles are positively charged and electrostatic contributions as well as chemical contributions contribute to As(V) adsorption. Above the isoelectric point, both the As(V) species and the FeOOH surface are negatively charged and adsorption is less favorable [14]. Therefore, arsenic is removed by co-precipitation of iron arsenate (Eqs. (12)–(15)) or adsorption (Eq. (16)), where the surface symbols $\equiv$ is used to denote the bonds of the cations with the surface of the solid. The symbol "|" as with $Fe(OH)_{2(s)}$ represents a surface bidentate complex and arsenate generally forms bidentate-binuclear bridging complexes [9,17,20].

$$2H_2O + AsO_4^{3-} + Fe^{3+} \rightarrow FeAsO_4.2H_2O \tag{12}$$

$$2FeOOH_{(s)} + H_2AsO_4^- \rightarrow (FeO)_2HAsO_4^- + H_2O + OH^- \tag{13}$$

$$3FeOOH_{(s)} + HAsO_4^{2-} \rightarrow (FeO)_3AsO_{4(s)}^- + H_2O + 2OH^- \tag{14}$$

$$\equiv Fe|(OH)_{2(s)} + HAsO_{4(aq)}^{2-} \rightarrow \equiv Fe|O_2As(O)(OH)_{2(s)} + 2OH_{(aq)}^- \tag{15}$$

$$Fe(OH)_{3(s)} + AsO_4^{3-} \rightarrow [Fe(OH)_3*AsO_4^{3-}]_{(s)} \tag{16}$$
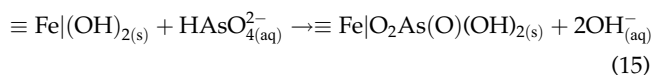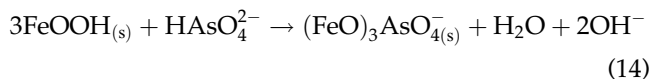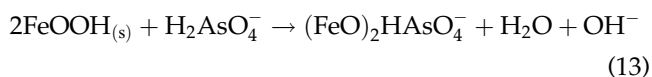
4. Results and discussion

4.1. Response surface methodology modeling results

Response surface methodology (RSM) is a collection of mathematical and statistical techniques, commonly used for improving and optimizing processes. It can be used to evaluate the relative significance of several affecting factors in the presence of complex interactions. When a combination of several independent variables and their interactions affect desired responses, RSM is an effective tool for optimizing the process [29]. Optimization of the process variables during wastewater treatment in the EC process can be achieved using RSM. Treatment of arsenic in wastewaters using different modeling approaches has been little investigated in literature [30–34].

Table 4
ANOVA results for the response parameters

Responses	R^2	Adj-R^2	S.D.	CV	F-value	Prob > F	AP
C_f (µg/L)	0.948	0.879	3.060	34.00	13.62	<0.0001	14.2
R_e (%)	0.944	0.869	2.990	3.28	12.55	<0.0001	15.1
ENC (kWh/m^3)	0.906	0.780	0.070	25.42	7.15	<0.0001	10.9
ELC (kg/m^3)	0.430	0.357	0.007	44.09	5.83	<0.0001	9.5
OC (€/m^3)	0.831	0.604	3.650	31.99	4.68	0.0005	8.7

In order to ensure the adequacy of the employed model, an adequate fit of the model should be given to avoid poor or ambiguous results. The significance of quadratic regression model was tested by the value of F, p, and R^2 and the corresponding results of analysis of variance (ANOVA) were tabulated in Table 4. The result of ANOVA was conducted to determine the significant effects of process variables on As(V) removal efficiency (R_e, %), effluent concentration (C_f), energy consumption (kWh/m^3), electrode consumption (kg/m^3), and operating cost (OC, $/m^3) for Fe ball anodes. F-values were 13.62, 12.55, and 4.68 for C_f, R_e, and OC for Fe ball anodes, respectively. The large F-values indicated that most of the variation in the response could be explained by the regression model equation. Values of Prob > F were less than 0.0001, which implied that the model was statistically significant. There is only 0.01% chance that a "Model F-Value" this large could occur due to noise. The model adequacies were checked by R^2 (0.94) and Adj-R^2 (0.87). A higher value of R^2 and Adj-R^2 for As(V) removal efficiency showed that the model could explain the response successfully. The coefficient of variance (CV) is the ratio of the standard error of estimate to the mean value of observed response (as percentage) and considered to be reproducible when it was not greater than 10%. In this work, the CVs for As(V) removal efficiency and operating cost were 3.28 and 31.99. Adequate precision (AP) measures the signal-to-noise ratio, and a ratio greater than 4.0 is desirable. For the present study, AP values for Fe ball anodes used in the EC process were 15.1 for R_e and 8.7 for OC, respectively, which indicated an adequate signal. The ANOVA indicated that the second-order polynomial model was significant and adequate to represent the actual relationship between the responses and the variables.

In the present study, the mathematical relationship between seven independent variables and responses was established well with the quadratic model. The quadratic regression model for R_e and OC from the Box–Behnken experiments in terms of coded values for Fe ball anodes in the EC process was presented in Eqs. (17) and (18):

$$
\begin{aligned}
R_e(\%) =\ & -226.88 + 40.43 \times \mathrm{pH}_i + 270.265 \times i + 56.92 \\
& \times t_{\mathrm{EC}} + 1.545 \times d_p + 0.074 \times C_o - 1.322 \times h \\
& + 14.99 \times Q_{\mathrm{air}} - 14.68 \times \mathrm{pH}_i \times i - 3.861 \times \mathrm{pH}_i \\
& \times t_{\mathrm{EC}} - 0.061 \times \mathrm{pH}_i \times d_p - 0.031 \times \mathrm{pH}_i \times C_o \\
& + 0.381 \times \mathrm{pH}_i \times h - 1.039 \times \mathrm{pH}_i \times Q_{\mathrm{air}} - 18.85 \\
& \times i \times t_{\mathrm{EC}} + 1.168 \times i \times d_p - 0.0126 \times i \times C_o \\
& - 4.333 \times i \times h - 1.442 \times i \times Q_{\mathrm{air}} - 0.229 \times t_{\mathrm{EC}} \\
& \times d_p + 9.625 \times 10^{-3} \times t_{\mathrm{EC}} \times C_o + 0.414 \times t_{\mathrm{EC}} \\
& \times h - 1.129 \times t_{\mathrm{EC}} \times Q_{\mathrm{air}} + 3.83.10^{-3} \times d_p \times C_o \\
& + 0.034 \times d_p \times h - 0.264 \times d_p \times Q_{\mathrm{air}} + 4.69 \\
& \times 10^{-3} \times C_o \times h + 5.669 \times 10^{-3} \times C_o \times Q_{\mathrm{air}} \\
& + 0.097 \times h \times Q_{\mathrm{air}} - 1.177 \times (\mathrm{pH}_i)^2 - 102.45 \\
& \times i^2 - 2.69 \times t_{\mathrm{EC}}^2 - 0.0197 \times d_p^2 + 2.655 \times 10^{-4} \\
& \times C_o^2 - 0.202 \times h^2 - 0.257 \times Q_{\mathrm{air}}^2
\end{aligned}
\tag{17}
$$

$$
\begin{aligned}
\mathrm{OC}\ \$/(\mathrm{m})^3 =\ & -6.81 \times 10^{-3} + 7.76 \times 10^{-3} \times \mathrm{pH}_i + 0.026 \\
& \times i - 9.51 \times 10^{-4} \times t_{\mathrm{EC}} + 4.59 \times 10^{-4} \times d_p \\
& + 1.06 \times 10^{-4} \times C_o - 4.462 \times 10^{-3} \times h \\
& - 3.408 \times 10^{-3} \times Q_{\mathrm{air}} + 5.56 \times 10^{-4} \times \mathrm{pH}_i \\
& \times i - 2.0 \times 10^{-5} \times \mathrm{pH}_i \times t_{\mathrm{EC}} - 1.70 \times 10^{-4} \\
& \times \mathrm{pH}_i \times d_p + 3.33 \times 10^{-6} \times \mathrm{pH}_i \times C_o \\
& + 9.48 \times 10^{-4} \times \mathrm{pH}_i \times h + 7.11 \times 10^{-4} \\
& \times \mathrm{pH}_i \times Q_{\mathrm{air}} + 0.145 \times i \times t_{\mathrm{EC}} - 1.11 \\
& \times 10^{-3} \times i \times d_p - 2.96 \times 10^{-4} \times i \times C_o \\
& - 5.56.10^{-4} \times i \times h - 1.25.10^{-3} \times i \times Q_{\mathrm{air}} \\
& - 4.0.10^{-5} \times t_{\mathrm{EC}} \times d_p - 6.90 \times 10^{-20} \times t_{\mathrm{EC}} \\
& \times C_o - 2.5 \times 10^{-5} \times t_{\mathrm{EC}} \times h + 4.38 \times 10^{-5} \\
& \times t_{\mathrm{EC}} \times Q_{\mathrm{air}} - 2.0 \times 10^{-6} \times d_p \times C_o - 3.33 \\
& \times 10^{-6} \times d_p \times h + 5.0 \times 10^{-6} \times d_p \times Q_{\mathrm{air}} \\
& + 3.33 \times 10^{-6} \times C_o \times h - 3.33 \times 10^{-6} \times C_o \\
& \times Q_{\mathrm{air}} - 2.52 \times 10^{-4} \times h \times Q_{\mathrm{air}} - 1.05 \\
& \times 10^{-3} \times (\mathrm{pH}_i)^2 + 1.72 \times 10^{-4} \times i^2 + 4.25 \\
& \times 10^{-4} \times t_{\mathrm{EC}}^2 + 6.21 \times 10^{-5} \times d_p^2 + 1.83 \\
& \times 10^{-6} \times C_o^2 - 1.21 \times 10^{-4} \times h^2 - 4.82 \\
& \times 10^{-5} \times Q_{\mathrm{air}}^2
\end{aligned}
\tag{18}
$$
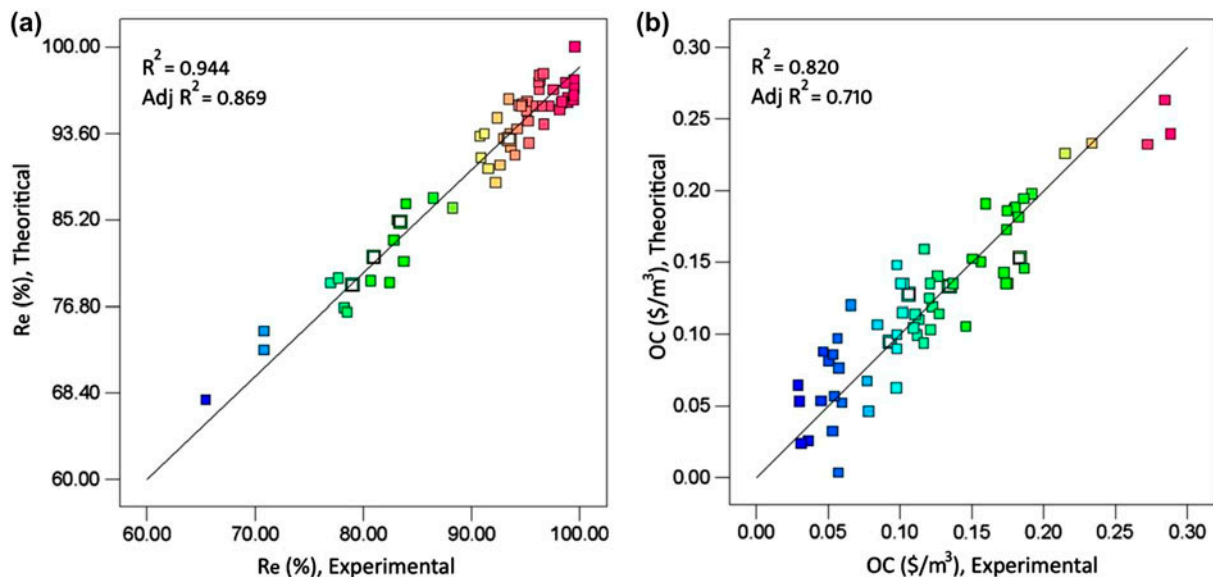
Fig. 2. Comparisons of predicted-experimental values for (a) removal efficiency of As(V) and (b) operating cost in the EC process.

Positive and negative signs in front of the terms referred to a synergistic effect and an antagonistic effect, respectively. The actual and the predicted removal efficiencies of As(V) in the EC process using Fe ball anodes were shown in Fig. 2. Actual values were the measured response data for a particular run, and the predicted values were obtained from the model. It was seen in the figure that the data points lay close to the diagonal line and the developed model was adequate for the prediction of each response. The value of predicted multiple correlation coefficient ($R^2 = 0.94$) for all responses is reasonable in agreement with the value of adjusted multiple correlation coefficient (Adj-$R^2 = 0.87$; Fig. 2). The fair correlation coefficients might be related to selection of variables in wide ranges with a limited number of experiments as well as the nonlinear influence of the investigated parameters on process response [35].

As seen from the ANOVA results, all the p-values for variables; x_1, x_2, x_3, x_7, (x_1x_2), (x_1x_3), (x_1x_7), x_2x_3, (x_2x_6), (x_4x_7), x_2^2, x_3^2, x_6^2 and x_7^2 for As(V) removal efficiency, x_3, x_5, (x_1x_2), (x_2x_3) and (x_1x_7) for operating cost and x_1, x_2, x_3, x_5, x_7, $x_1 x_2$, $x_1 x_3$, $x_1 x_7$, $x_2 x_3$, $x_2 x_5$, $x_2 x_6$, $x_3 x_5$, $x_3 x_7$, $x_4 x_7$, x_2^2, x_3^2, x_6^2, x_7^2 for effluent As(V) concentration were less than 0.05 which indicated that these variables were significant and had great influence on the removal efficiency in the EC process. The analysis showed that the form of the model chosen for this study to explain the relationship between the variables and the responses was correct and could be used to navigate the design space.

Effects of independent process variables for the removal of As(V) in the EC process were evaluated with results of perturbation graph from the Design-Expert software (Fig. 3). The removal efficiency increased with operating parameters namely, pH$_i$, i, t_{EC}, Q_{air}, and h to the center point, and then they
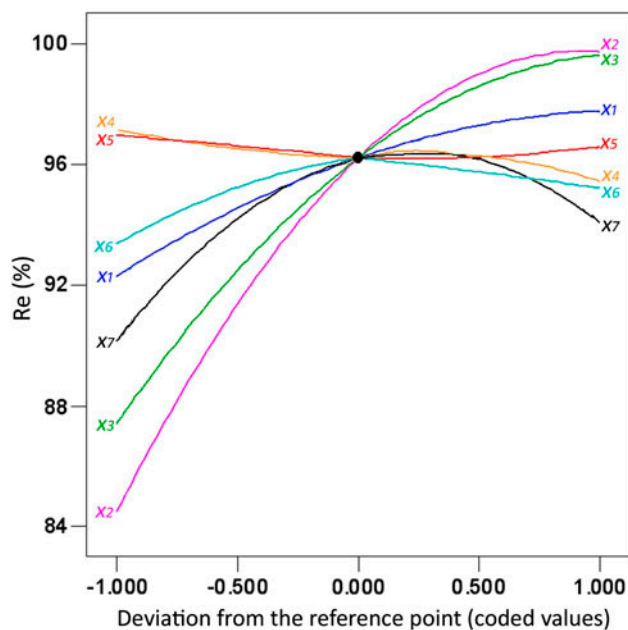
Fig. 3. Perturbation graph of As(V) removal with respect to independent variables.

decreased slowly apart from current and t_{EC}. The highest effects on the removal efficiency of As(V) were observed with the applied current and operating time. At higher current, higher dissolution of electrode material (Eq. (2)) with higher rate of formation of iron hydroxides and some polymeric metal complexes resulted in higher removal efficiency of arsenic due to co-precipitation.

Contour plots were drawn as a function of two factors at a time, holding all other factors at fixed levels (normally at the zero level). Those plots were helpful in understanding both the main and the interaction effects of these two factors (Fig. 4). Responses such as the removal of As(V) efficiency and operating cost with respect to the independent process variables were listed for each run in Table 2. The As(V) removal
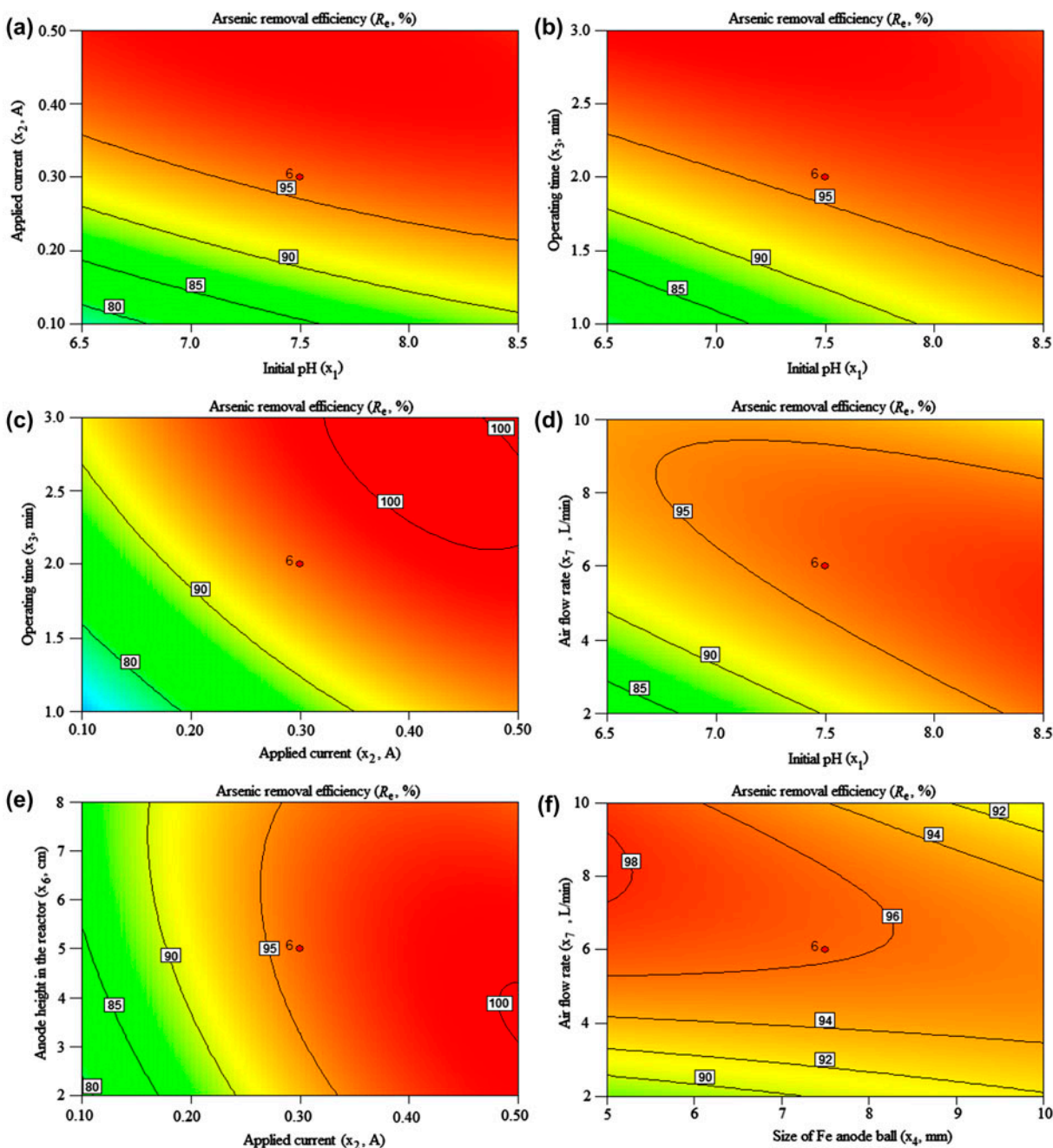
Fig. 4. Contour plots for removal of As(V) from groundwater by the EC process using Fe ball anodes.

efficiency increased from 95.3 at 0.1 A to 99.5% at 0.5 A (runs 62 and 57). The similar removal efficiency trend was observed for runs 9 and 10 (Table 2). This indicated that As(V) removal efficiency at pH_i 7.5 was higher than that of pH_i 6.5 which was depicted in Figs. 4(a) and 5. When interaction of $pH_i \times i$ was considered with based on the above results, there was not much higher removal efficiency observed beyond pH_i 7.5 as the applied current increased further (Fig. 4(a)). The other parameter affected for the removal process was the operating time. The removal efficiency increased from 70.8% at 1 min (run 53) to 95.3% at 3 min (run 62, Table 2). Similar results were obtained with runs 49 and 20 (83.8% at 1 min and 99.6% at 3 min). This referred that the removal efficiency increased with increasing of operating time. As seen in Fig. 4(b), the removal efficiency also decreased with increasing of both pH_i and t_{EC}, but the removal efficiency increased only with increasing of operating time at constant pH_i. Two of the most important parameters on removal of As(V) in the EC process were current and operating time, since the Faraday's law controls amount of dissolution of Fe anode ball (Eq. (2)). When the dissolved amount of Fe ball anode increased with increase in i and t_{EC}, then the removal efficiency increased. The removal efficiency at the applied current of 0.5 A was 95.2% at 1 min (run 1) and 99.6% at 3 min (run 22) when the experimental conditions were pH_i 7.5, 7.5 mm ball size, 100 μg/L, column height of 2 cm, and 6 L/min. As the operating time was kept constant at 1 min, the removal efficiency was 70.8% at 0.1 A (run 53) and 91.6% at 0.5 A (run 17). When the applied current to surface of anode ball increased, the amount of dissolution of anode material increased which resulted in the increase amount of As(V) in solution. As(V) removal efficiency increased to 100% at

0.4 A and 2.5 min because the removal efficiency increased with increasing of i and t_{EC} (Figs. 4(c) and 5(b)).

As(V) removal efficiency increased with increasing of Q_{air} at lower pH values and the removal decreased as both pH_i and Q_{air} increased (Fig. 4(d)). As an example, the removal efficiency at constant pH 6.5 increased from 77.1% at 2 L/min to 93.6% at 10 L/min (runs 50 and 26, Fig. 6). Moreover, Fe^{2+} ion released from the dissolution of anode was oxidized to Fe^{3+} with oxygen in aqueous solution (Eqs. (19) and (20))

$$4Fe^{2+} + O_{2(aq)} + 2H_2O + 8OH^- \rightarrow 4Fe(OH)_{3(s)} \quad (19)$$

$$4Fe^{2+} + O_{2(aq)} + +6H_2O \rightarrow 4FeOOH_{(s)} + 8H^+ \quad (20)$$
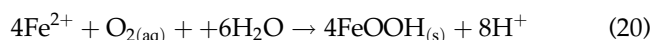
Fe^{2+} oxidation was very slow at pH < 6.5 during the EC process (5 h), but Fe^{2+} oxidation was noticed faster at pH 7.5 (10 min) [36]. Iron species in the solution at this pH_i were probably Fe(II) and $Fe(OH)_{3(s)}/FeOOH_{(s)}$. At pH 8.5, the oxidation took place in a very short time and the species were $Fe(OH)_{3(s)}/FeOOH_{(s)}$. Concentration of dissolved oxygen in the solution was 8.5 mg/L which might contribute to the oxidation of Fe^{2+} to Fe^{3+}, and Fe^{2+} concentration was reduced as pH_i increased. Fe^{2+} concentration at low pH values in the solution did not affect the arsenic adsorption capacity.

The other parameter that affected for the removal of As(V) was Fe ball size. The removal efficiency varied from 95.4% at 5 mm (run 8) to 84.1% at 10 mm (run 14). The removal efficiency changed from 91.4% at 10 mm (run 6) to 99.5% at 5 mm (run 15). As the anode ball size increased, the removal efficiency decreased. In other words, the removal rate increased
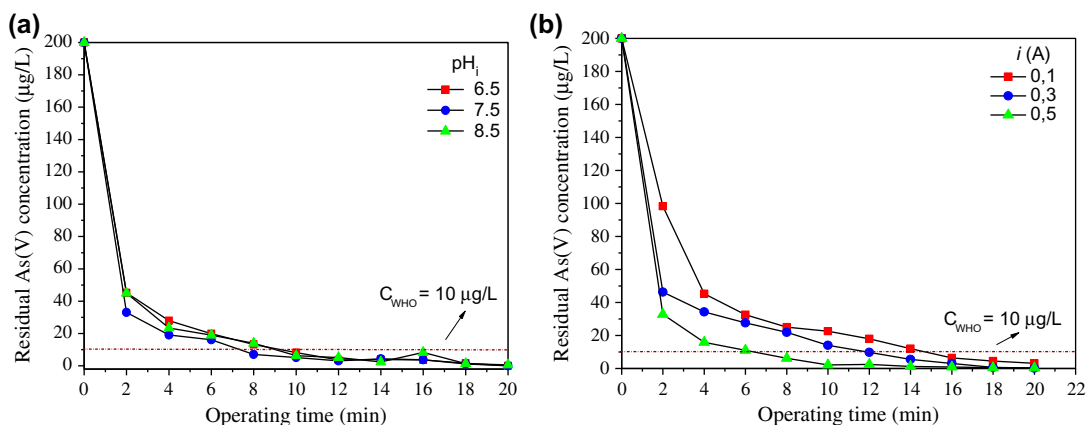
Fig. 5. Effects of (a) pH_i and (b) applied current on the removal efficiency of As(V) in the EC process (0.3 A, column height of 5.0 cm, 7.5 mm ball size, and 6 L/min).
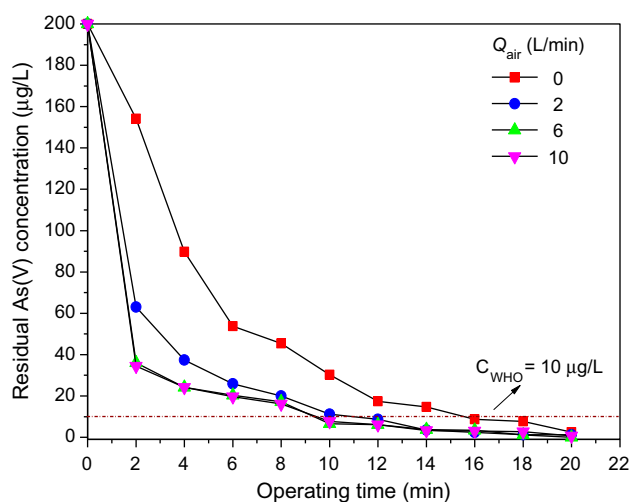
Fig. 6. Effect air flow rate on the removal efficiency of As (V) in the EC process (0.3 A, column height of 5.0 cm, and 5 mm ball size).

with increasing of electrochemical active surface area of anode ball (Table 2 and Fig. 7(a)). The removal efficiency within 1 min at the same experimental conditions (pH$_i$ 7.5, 7.5 mm ball size, 0.1 A, 100 μg/L, and 6 L/min) except for the column height in the EC reactor was 60.5% at 2 cm and 70.8% at 8 cm (runs 44 and 53), and the removal efficiency in 3 min was 83.5% at 2 cm and 95.3% at 8 cm (runs 56 and 62). The removal efficiencies at constant column height of 8 cm were 70.8% at 0.1 A, 91.6% at 0.5 A (runs 53 and 17), and 83.5% at 0.1 A and 2 cm column height and 99.6% at 0.5 A and 2 cm column height (runs 56 and 22). As values of h and i increased, the removal efficiency increased due to the interaction of $h \times i$. The similar effect was observed with increasing of column height

at constant applied current (Fig. 4(e)). In addition, Fig. 7(b) also supported that the removal efficiency increased with the increase in the column height along the operating time in the EC reactor. When column height was 2 cm in the EC reactor, total surface areas of Fe ball anode for sizes of 5.0, 7.5, and 10 mm were 0.03297, 0.03179, and 0.0157 m^2. Total surface areas for 5 mm ball anode with column heights of 2, 5, and 8 cm were 0.03297, 0.06986, and 0.13188 m^2. This explained that total surface area of the anode decreased with the ball size increase at constant column height in the EC reactor or total surface area of the anode increased as the column height increased at constant ball size in the EC reactor.

Fig. 4(f) illustrated the effect of interaction $d_p \times Q_{air}$ on the As(V) removal in the EC process. The removal efficiency was obtained as 99.6% for 5 mm ball size and 96.3% for 10 mm ball size at 6 L/min (run 10 and 51). In addition, the similar result at 2 L/min was obtained as 99.5% at 5 mm ball size and 91.4% at 10 mm ball size (run 15 and 6). As the anode ball size from 5 mm to 10 mm at 10 L/min increased, the removal efficiency varied from 95.4 to 84.1%. The highest removal efficiency was determined when air flow rate and anode ball size were 6 L/min and 5 mm (Fig. 4(f)). Concentration of As(V) in the solution also affected the removal efficiency in the EC process. The removal efficiency changed from 98.3% at 50 μg/L to 91.2% at 150 μg/L (runs 13 and 60). A similar trend was obtained for the removal as 98.2% at 50 μg/L and 90.9% at 150 μg/L (runs 16 and 61), respectively. Contour plots in Fig. 4 revealed that As(V) removal efficiency in the EC process increased with an increase in applied current, operating time, and column height of Fe ball in the EC reactor except for Fe ball size.
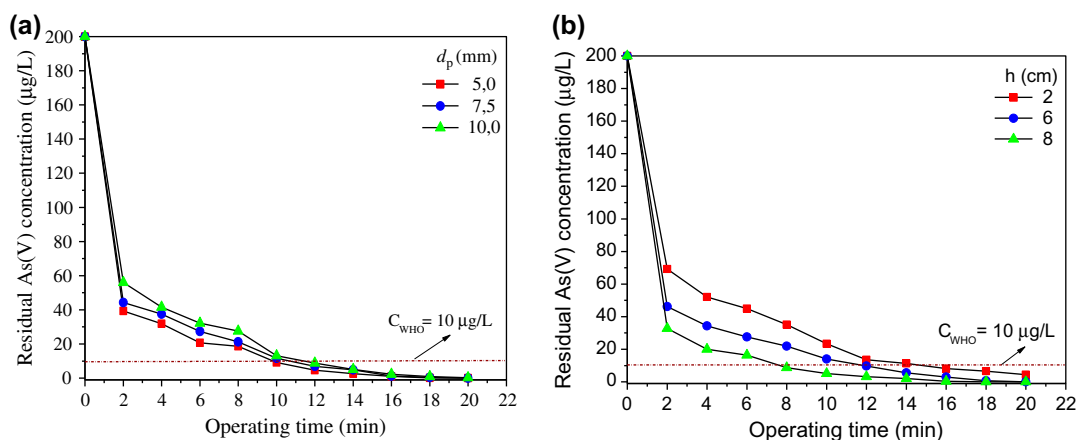
Fig. 7. Effects of (a) Fe ball anode size and (b) column height in the EC reactor on the removal efficiency of As(V) in the EC process (pH$_i$ 7.5, 0.3 A, and 6 L/min).

4.2. Optimization of operating conditions

Optimization process variables and responses with four criteria for the removal of As(V) from groundwater were presented in Table 5 as the other operating variables are in range. As can be seen in Table 5, the quadratic model produced the optimization results at 100 µg/L for the minimum effluent concentration, maximum removal efficiencies, and minimum operating cost as 0.4 µg/L, 99.2%, and 0.031 $/m^3. Final effluent concentration for case (e) was selected as 9.9 µg/L since the recommended arsenic concentration of drinking water is set to 10 µg/L by WHO.

4.3. Confirmation experiments

Further to support the validity of the statistical experimental design, some additional confirmation experiments were conducted. The chosen conditions were all listed in Table 6, along with the predicted and measured results. As shown in Table 6, the observed values of effluent concentrations, removal efficiencies, and operating costs were close to those predicted values obtained from the model. This also testified that the model approach was appropriate for optimizing the operational conditions for the removal of As(V) from groundwater.

Table 5
Optimization process variables and responses for the removal of As(V) using iron ball anode electrodes

	Variables							Responses		
Criteria for responses	pH_i (−)	i (A)	t_{EC} (min)	d_p (mm)	C_o (µg/L)	h (cm)	Q_{air} (L/min)	C_f (µg/L)	R_e (%)	OC ($/m^3)
I[a]	7.6	0.48	1.1	7.7	104	2.3	6.3	4.3	96.2	0.035
II[b]	7.5	0.27	1.1	5.3	107	4.8	9.6	9.9	91.1	0.077
III[c]	8.5	0.48	1.1	6.7	53.9	5.9	5.8	0.5	99.6	0.028
IV[d]	7.0	0.50	1.1	5.0	150	2.0	8.5	5.5	98.5	0.030
V[e]	7.2	0.50	1.2	5.0	100	4.8	9.9	0.4	99.2	0.031

Notes: (a) C_f (minimum), R_e (in range) and OC (in range), (b) C_f = 9.9 µg/L, R_e (in range) and OC (in range), (c) C_f (minimum), R_e (maximum) and OC (minimum), (d) C_f (minimum), R_e (maximum) and OC (minimum), and (e) C_f (minimum), R_e (maximum), and OC (minimum).

Table 6
Predicted and observed values for the confirmation experiments

	Independent variables							Responses					
								C_f (µg/L)		R_e (%)		OC ($/m^3)	
Run No	x_1: pH_i	x_2:i	x_3: t_{EC}	x_4: d_p	x_5: C_o	x_6: h	x_7: Q_{air}	Predicted	Observed	Predicted	Observed	Predicted	Observed
1	7.0	0.15	3	7.5	150	5	2	15.76	17.89	89.75	90.74	0.1742	0.1524
2	7.0	0.15	2	7.5	150	8	10	7.54	8.01	96.45	95.66	0.1560	0.1654
3	7.0	0.25	3	7.5	150	5	6	3.17	5.244	99.98	98.50	0.2022	0.2275
4	7.0	0.25	1	5.0	50	5	2	3.46	5.69	94.39	93.62	0.2173	0.1945
5	7.0	0.40	2	10.0	150	5	2	0.686	0.715	99.86	99.52	0.1658	0.1755
6	7.0	0.40	1	5.0	50	2	6	0.285	0.538	99.43	98.92	0.1777	0.1548
7	6.5	0.15	1	5.0	50	5	6	2.15	2.12	95.70	95.75	0.1694	0.1506
8	6.5	0.15	2	10.0	100	5	2	14.03	17.40	86.39	85.60	0.1748	0.1525
9	6.5	0.25	2	7.5	100	5	6	2.71	1.02	97.62	98.98	0.2017	0.1901
10	6.5	0.25	3	10.0	150	8	6	4.85	5.98	99.93	99.01	0.1751	0.1564
11	6.5	0.40	2	7.5	100	5	10	1.304	0.476	98.85	99.52	0.2013	0.1742
12	8.0	0.15	1	10.0	50	5	2	4.68	5.248	88.93	89.50	0.1304	0.1365
13	8.0	0.25	1	10.0	100	8	6	5.97	6.365	94.97	93.64	0.1038	0.0990
14	8.0	0.25	2	7.5	100	2	10	13.90	14.71	86.29	85.29	0.0965	0.0878
15	8.0	0.25	3	5.0	150	5	6	1.50	2.582	99.09	98.28	0.2111	0.1955
16	8.0	0.40	3	5.0	100	2	2	4.58	3.96	96.55	96.04	0.2093	0.1879

4.4. Comparison of performances of plate type and ball type of electrode

The arsenic removal reported with the plate-type electrode at initial arsenic concentration of 150 µg/Lin the earlier study was compared with Fe ball used in the air fed EC reactor [9]. The highest arsenic removal efficiencies achieved with Fe ball and plate type of electrodes at the same initial concentration as 98.5% at pH 7.0, 0.5 A, 1.1 min, 5 mm ball size, column height of 2 cm, 8.5 L/min, effluent concentration of 5.5 µg/L and 94.1% at pH 6.5, 5 A/m^2, 7.5 min, effluent concentration of 8.9 µg/L for monopolar parallel electrode connection mode (MP-P); 98.3% at pH 6.5, 7.5 A/m^2, 2.5 min, effluent concentration of 2.5 µg/L for monopolar series electrode connection mode (MP-S) and 98.4% at pH 6.5, 7.5 A/m^2, 2.5 min, effluent concentration of 2.4 µg/L for bipolar series electrode connection mode (BP-S), respectively. The operating costs at the optimum operating conditions were calculated as 0.030 $/m^3 for air fed EC reactor and 0.035 $/m^3 for MP-P, 0.026 $/m^3 for MP-S, and 0.035 $/m^3 for BP-S. Performance of iron ball electrodes in the air fed reactor was found to be as good as plate-type electrode in the EC reactor, but some design elements in the air fed reactor need to improve in order to achieve a better performance for the future studies.

5. Conclusions

In this study, the Box–Behnken statistical experiment design is applied to optimize the removal efficiency of As(V) from groundwater by EC with Fe ball anodes. The statistical experiment design involved seven important operating variables: initial pH$_i$, current, operating time, size of iron ball anode, initial As(V) concentration, column height in the EC reactor, and air flow rate on the removal efficiency of As(V) in the EC process. The total 62 experiments were conducted in the present study for construction of a quadratic model. Very high regression coefficient > 0.94 between the variables and the response indicated excellent evaluation of experimental data by quadratic model. Among the factors, operating time and current have positive effect on As(V) removal. Using the new EC reactor in the EC process resulted in 99.2% for removal efficiency of As(V), operating cost of 0.031 $/m^3, and effluent concentration of 0.4 µg/L for initial concentration of 100 µg/L at the optimized conditions. Thus, the results presented in this work indicated that EC can be effectively used for the removal of low concentrations of As(V) in groundwaters.

References

[1] P.L. Smedley, D.G. Kinniburgh, A review of the source, behaviour and distribution of arsenic in natural waters, Appl. Geochem. 17 (2002) 517–568.

[2] P. Ravenscroft, H. Brammer, K. Richards, Arsenic pollution: A Global Synthesis. RGS-IBG Book Series, A John Wiley and Sons, London, 2009.

[3] B.K. Mandal, K.T. Suzuki, Arsenic round the world: A review, Talanta 58 (2002) 201–235.

[4] M.M. Rahman, J.C. Ngm, R. Naidu, Chronic exposure of arsenic via drinking water and its adverse health impacts on humans, Environ. Geochem. Health 31 (2009) 189–200.

[5] World Health Organization, Guidelines for Drinking Water Quality, third ed., vol. 1, WHO Press, Geneva, 2004.

[6] M. Colak, U. Gemici, G. Tarcan, The effects of colemanite deposits on the arsenic concentrations of soil and ground water in Igdekoy-Emet, Kutahya, Turkey, Water Air Soil Pollut. 149 (2003) 127–143.

[7] U. Gemici, G. Tarcan, C. Helvacı, A.M. Somay, High arsenic and boron concentrations in groundwaters related to mining activity in the Bigadic borate deposits (western Turkey), Appl. Geochem. 23 (2008) 2462–2476.

[8] O. Gunduz, C. Simsek, A. Hasozbek, Arsenic pollution in the groundwater of Simav Plain, Turkey: Its impact on water quality and human health, Wat. Air Soil Pollut. 205 (2010) 43–62.

[9] M. Kobya, U. Gebologlu, F. Ulu, S. Oncel, E. Demirbas, Removal of arsenic from drinking water by the electrocoagulation using Fe and Al electrodes, Electrochim. Acta 56 (2011) 5060–5070.

[10] M. Vaclavikova, G.P. Gallios, S. Hredzak, S. Jakabsky, Removal of arsenic from water streams: An overview of available techniques, Clean Technol. Environ. Policy 10 (2008) 89–95.

[11] M. Kobya, E. Demirbas, O.T. Can, M. Bayramoglu, Treatment of levafix orange textile dye solution by electrocoagulation, J. Hazard. Mater. 132 (2006) 183–188.

[12] M. Kobya, E. Demirbas, N.U. Parlak, S. Yigit, Treatment of cadmium and nickel electroplating rinse water by electrocoagulation, Environ. Technol. 31 (2010) 1471–1481.

[13] M. Kobya, F. Ulu, U. Gebologlu, E. Demirbas, M.S. Oncel, Treatment of potable water containing low concentration of arsenic with electrocoagulation: Different connection modes and Fe-Al electrodes, Sep. Purif. Technol. 77 (2011) 283–293.

[14] W. Wan, T.J. Pepping, T. Banerji, S. Chaudhari, D.E. Giammar, Effects of water chemistry on arsenic removal from drinking water by electrocoagulation, Water Res. 45 (2011) 3843–4392.

[15] D. Lakshmanan, D.A. Clifford, G. Samanta, Comparative study of arsenic removal by iron using electrocoagulation

and chemical coagulation, Water Res. 44 (2010) 5641–5652.

[16] N.S. Kumar, S. Goel, Factors influencing arsenic and nitrate removal from drinking water in a continuous flow electrocoagulation (EC) process, J. Hazard. Mater. 173 (2010) 528–533.

[17] J.A.G. Gomes, P. Daida, M. Kesmez, M. Weir, H. Moreno, J.R. Parga, G. Irwin, H. McWhinney, T. Grady, E. Peterson, D.L. Cocke, Arsenic removal by electrocoagulation using combined Al-Fe electrode system and characterization of products, J. Hazard. Mater. 139 (2007) 220–231.

[18] J.R. Parga, D.L. Cocke, J.L. Valenzuela, J.A. Gomes, M. Kesmez, G. Irwin, H. Moreno, M. Weir, Arsenic removal via electrocoagulation from heavy metal contaminated groundwater in La Comarca Lagunera Mexico, J. Hazard. Mater. 124 (2005) 247–254.

[19] P.R. Kumar, S. Chaudhari, K.C. Khilar, S.P. Mahajan, Removal of arsenic from water by electrocoagulation, Chemosphere 55 (2004) 1245–1252.

[20] H.K. Hansen, P. Nunez, C. Jil, Removal of arsenic from wastewaters by airlift electrocoagulation. Part 1: Batch reactor experiments, Sep. Sci. Technol. 43 (2008) 212–224.

[21] H.K. Hansen, P. Nunez, C. Jil, Removal of arsenic from wastewaters by airlift electrocoagulation. Part 2: Continuous reactor experiments, Sep. Sci. Technol. 43 (2008) 3663–3675.

[22] H.K. Hansen, P. Nunez, D. Raboy, I. Schippacasse, R. Grandon, Electrocoagulation in wastewater containing arsenic: Comparing different process designs, Electrochim. Acta 52 (2007) 3464–3470.

[23] N. Balasubramanian, T. Kojima, C.A. Basha, C. Srinivasakannan, Removal of arsenic from aqueous solution using electrocoagulation, J. Hazard. Mater. 167 (2009) 966–969.

[24] M. Kobya, E. Demirbas, A. Dedeli, M.T. Sensoy, Treatment of rinse water from zinc phosphate coating by batch and continuous electrocoagulation processes, J. Hazard. Mater. 173 (2010) 326–334.

[25] M. Kobya, H. Hiz, E. Senturk, C. Aydiner, E. Demirbas, Treatment of potato chips manufacturing wastewater by electrocoagulation, Desalination 190 (2006) 201–211.

[26] APHA (American Public Health Association), Standard Methods for the Examination of Water and Wastewater, twentieth ed., American Public Health Association, Washington, DC, 1998.

[27] M. Kobya, E. Demirbas, A. Akyol, Electrochemical treatment and operating cost analysis of textile wastewater with iron electrodes, Water Sci. Technol. 60 (2009) 2261–2270.

[28] J.F. Martinez-Villafane, C. Montero-Ocampo, A.M. Garcia-Lara, Energy and electrode consumption analysis of electrocoagulation for the removal of arsenic from underground water, J. Hazard. Mater. 172 (2009) 1617–1622.

[29] R.H. Myers, D.C. Montgomery, Response Surface Methodology: Process and Product Optimization Using Designed Experiments, second ed., John Wiley and Sons, New York, NY, 2002.

[30] M. Kobya, E. Demirbas, M. Bayramoglu, M.T. Sensoy, Optimization of electrocoagulation process for the treatment of metal cutting wastewaters with response surface methodology, Water, Air Soil Pollut. 215 (2011) 399–410.

[31] M. Kobya, E. Demirbas, U. Gebologlu, M.S. Oncel, Y. Yildirim, Optimization of arsenic removal from drinking water by electrocoagulation batch process using response surface methodology, Desalin. Water Treat. 51 (2013) 6676–6687.

[32] D. Prabhakaran, C.A. Basha, T. Kannadasan, P. Aravinthan, Removal of hydroquinone from water by electrocoagulation using flow cell and optimization by response surface methodology, J. Environ. Sci. Health-A 45 (2010) 400–412.

[33] I. Arslan-Alaton, M. Kobya, A. Akyol, M. Bayramoglu, Electrocoagulation of azo dye production wastewater with iron electrodes: Process evaluation by multi-response central composite design, Color. Technol. 125 (2009) 234–241.

[34] T. Ölmez, The optimization of Cr(VI) reduction and removal by electrocoagulation using response surface methodology, J. Hazard. Mater. 162 (2009) 1371–1378.

[35] N. Aktas, I.H. Boyaci, M. Mutlu, A. Tanyolac, Optimization of lactose utilization in deproteinated whey by Kluyveromyces marxianus using response surface methodology (RSM), Bioresour. Technol. 97 (2006) 2252–2259.

[36] D. Lakshmanan, D.A. Clifford, G. Samanta, Ferrous and ferric ion generation during iron electrocoagulation, Environ. Sci. Technol. 43 (2009) 3853–3859.